Engineering Geology 293 (2021) 106299

Contents lists available at ScienceDirect

Engineering Geology

journal homepage: www.elsevier.com/locate/enggeo

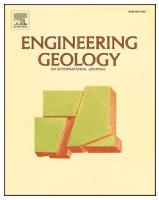

Exploring the effects of temperature on intrinsic permeability and void ratio alteration through temperature-controlled experiments

Mohammad Joshaghani , Omid Ghasemi-Fare *

Department of Civil and Environmental Engineering, University of Louisville, Louisville, USA

ARTICLE INFO

Keywords:
Hydraulic conductivity
Intrinsic permeability
Temperature-controlled triaxial permeameter
Thermal loading
Thermal volume change

ABSTRACT

An increase in temperature changes the groundwater density and viscosity, therefore, it is expected that the soil hydraulic conductivity varies with temperature. Beyond this point, thermal loading induces volumetric changes for both sand and clay and may alter soil fabric. These variations might increase or decrease the intrinsic permeability of the soil. A modified temperature-controlled triaxial permeameter cell was used in this study to elevate soil temperature from 20 °C to 80 °C. Moreover, the setup was designed to control the temperature and pressure of the permeant water injected into the specimen. The hydraulic conductivity of both Ottawa sand and Kaolin clay under different confinement stresses (69 kPa to 690 kPa) was measured. Then, intrinsic permeability was calculated considering water properties variation with temperature. The results determined that, although hydraulic conductivity increases with temperature for both Ottawa sand and Kaolin clay, the intrinsic permeability of Ottawa sand reduces by 50%, while in Kaolin clay it slightly reduces when the temperature rises from 20 °C to 80 °C. Nonetheless, analyzing volumetric changes and void ratio variations for both selected soil types show a reduction in void ratio with temperature. Reduction in the void ratio can explain the lower intrinsic permeability in Ottawa sand at the elevated temperature, however in Kaolin clay despite the higher void ratio reduction, another mechanism which is the degeneration of a part of the immobile water within the structure into the mobile water plays an important role.

1. Introduction

Permeability is one of the most important soil properties which controls the seepage and water movement in the ground and directly, or indirectly underpins many geotechnical problems such as slope stability analysis and landfill designs (Damiano et al., 2017; Dou et al., 2014; Jefferson and Rogers, 1998; Ng and Leung, 2012; Sadeghi and AliPanahi, 2020). Accurate prediction of soil permeability and its variation with temperature is necessary to accurately model energy geostructures, waste disposals, and landfill covers subjected to daily temperature variations (Campanella and Mitchell, 1968; Garakani et al., 2015; Ghasemi-Fare and Basu, 2018; Joshaghani and Ghasemi-Fare, 2019). Thermal loading alters soil and fluid properties (Cherati and Ghasemi-Fare, 2019; Monfared et al., 2014; Tamizdoust and Ghasemi-Fare, 2020a). Therefore, to properly understand the thermo-hydro-mechanical (THM) response of the geotechnical infrastructures, the variations of the soil properties (e.g., permeability) with temperature must be investigated (Chen et al., 2017; François et al., 2009; Ghasemi-Fare and Basu, 2019; Tamizdoust and Ghasemi-Fare, 2020b). In most of the previous research changes in hydraulic properties (e.g., hydraulic conductivity) of both coarse and fine-grained soils with temperature were mainly considered due to the fluid properties (density, and viscosity of the water) alteration (Cho et al., 1999; Delage et al., 2000; Ghasemi-Fare and Basu, 2015; Gobran et al., 1987; Sageev, 1980). Nevertheless, recently there have been studies that showed the measured hydraulic conductivity (H·C.) values at elevated temperatures are different from the calculated values by only considering the updated viscosity and density of the water at the selected temperatures (Gao and Shao, 2015; Ye et al., 2012; Ye et al., 2013). Therefore, both hydraulic conductivity and intrinsic permeability are expected to change with temperature alterations.

2. Review of existing models

There have been several attempts in the literature to predict the soil hydraulic conductivity and intrinsic permeability variations with temperature using indirect (Habibagahi, 1977; Morin and Silva, 1984; Towhata et al., 1993) or direct measurements (Cho et al., 1999;

* Corresponding author.
E-mail addresses: m.joshaghani@louisville.edu (M. Joshaghani), omid.ghasemifare@louisville.edu (O. Ghasemi-Fare).

https://doi.org/10.1016/j.enggeo.2021.106299
Received 27 October 2020; Received in revised form 15 July 2021; Accepted 21 July 2021
Available online 24 July 2021

Derjaguin et al., 1986; Gobran et al., 1987; Joshaghani and Ghasemi-Fare, 2019; Joshaghani et al., 2018). The indirect method is referred to as the back-calculation of hydraulic conductivity from consolidation tests at different temperatures. However, different behaviors (e.g., reduction, increase, and no changes in permeability) were reported in the literature for both sand and clays. Habibagahi (1977) observed an increase in derived hydraulic conductivity with temperature on silty clay. Derjaguin et al. (1986) and Pusch (1992) reported that when the temperature increases, gaps in the soil can be filled more easily, and then water channels would form. Therefore, it could be concluded that in a more condensed medium, these channels form readily and more changes in intrinsic permeability happen by an expansion of the soil skeleton. In another study, Towhata et al. (1993) measured H.C. of MC clay (artificial Kaolin clay) and bentonite at different temperatures and observed higher values for measured H.C. compared to the calculated values using only the updated fluid properties at elevated temperatures. They suggested that the degeneration of adsorbed water into the free water accounts for this observation. In another study, Seiphoori (2015) reported that the degeneration of a part of the immobile water within the structure into the mobile water causes the increase in intrinsic permeability of bentonite at elevated temperatures. On the other hand, Romero et al. (2001), and Villar and Lloret (2004), respectively, measured H.C. for Boom clay, and bentonite at different temperatures and reported that soil densification due to thermal consolidation, and clay fabric changes cause a reduction in intrinsic permeability at elevated temperatures. In a recent study, Chen et al. (2017) reported that the microstructure weakening effect due to the thermal volume change resulted in intrinsic permeability reduction in Boom clay. In contrast to the aforementioned studies, Delage et al. (2009) performed temperature-controlled constant head permeability tests on Boom clay and observed a 148% increase in hydraulic conductivity of the Boom clay when the temperature rises from 20 °C to 90 °C. While they reported no changes in intrinsic permeability in the selected temperature range by considering the alteration in dynamic viscosity of the water according to the experimental measurements reported in the literature (Hillel, 2013). In another study, Ren et al. (2014) reported that for a temperature range between 10 °C and 25 °C intrinsic permeability of silty clay can increase or decrease depending on the dry bulk density.

Similar to clayey soils, different behaviors were reported in the literature about the effect of temperature on the coarse-grained soil properties. Several studies showed that the changes in intrinsic permeability are insignificant with temperature variations for cemented quartz samples and unconsolidated Ottawa sand at different confining pressures and indicated insignificant thermal volume change in sandy soils (Arihara, 1974; Gobran et al., 1987; Greenberg et al., 1968; Leung et al., 2020; Sageev, 1980). While a reduction (Aruna, 1977; Weinbrandt et al., 1975) and an increase in soil permeability (Aktan and Ali, 1975; Somerton and Gupta, 1965) of coarse-grained soil with temperature were reported in other studies.

Different observations on the amount of thermal volume change (or porosity change) and permeability values at elevated temperatures are reported in the literature. In addition, most of the previous researches indicated that the effect of temperature on sandy soil properties (e.g., permeability and volumetric strain) are minor. Besides, the effect of temperature on the intrinsic permeability of sand and clays with different initial conditions (initial confinement or initial void ratio) has not been completely studied in the literature. Therefore, to address these issues, and to compare the effect of fluid properties variations and other mechanisms (e.g., particle rearrangement in sandy soil and thermal volume reduction, or degeneration of adsorbed water in clayey soils) the changes in H.C. with temperature of Ottawa sand and Kaolin clay at different confinement stresses (60 kPa to 690 kPa) were measured using a modified temperature-controlled triaxial permeameter cell. Then alterations in intrinsic permeability were calculated by utilizing measured fluid properties (e.g., dynamic viscosity) at each temperature. In the second phase of this research, the changes in the void ratio were measured during the thermal loading for both Ottawa sand and Kaolin clay.

3. Experimental setup

3.1. Test setup

To prepare the setup and perform hydraulic conductivity tests at different temperatures, a spiral cooper coil was embedded inside the permeameter cell to circulate a heat carrier fluid from the cooling/heating circulating bath. A type-*T* thermocouple was placed inside the cell and the second thermocouple was used to measure room temperature. Both thermocouples were connected to a six-channel handheld temperature data logger from Omega Co. Fig. 1 shows different parts of the modified permeameter cell. Fig. 1(a) illustrates the digital data logger which stores the temperature every two minutes in a memory card. Fig. 1(b) shows the modified temperature-controlled cell with an aluminum chamber and heat exchanger tubes (connected to the modified top cap). Fig. 1(c) shows the cell bottom cap with a sample inside a latex membrane. Please note, an extra thermocouple was inserted inside the specimen during the calibration tests which is not shown in Fig. 1. To perform H.C. of Ottawa sand, samples with 50.8 mm (2 in) diameter and 101.6 mm (4 in) height were selected, while for Kaolin clay tests, the diameter and height of the samples were, respectively, 101.6 mm (4 in) and 25.4 mm (1 in). Please note, according to the ASTM-D5084 shorter samples with larger diameters can be used for clayey soil which has lower permeability compared to coarse-grained soil to accelerate the flow and perform faster tests. The hydraulic conductivity test of Ottawa sand only took a few minutes while the same test would take at least 20 to 30 min for Kaolin clay.

Please note the setup (temperature-control triaxial permeameter cell) does not have any thermal insulation. In addition, there is a heat loss from the tubes which carry fluid from the water bath to the cell. Therefore, several calibration tests were conducted to correlate the temperature of the water bath based on the target temperature in the cell.

Since the heat-carrying fluid inside the coil flows continuously during the test and the setup is placed in a temperature control room, insulation was not necessarily required. During the first set of calibration tests, the relation between the water bath temperature and the temperature inside the cell and the specimen was obtained at all target temperatures. Please also kindly note, the thermocouple placed inside the cell was used to monitor the temperature every 5 s and the hydraulic conductivity tests have performed at all target temperatures while the cell temperature reaches the steady state condition (i.e. cell temperature and specimen temperature were equal) in almost 60 min.

A thermocouple was permanently placed inside the cell to control and monitor the cell temperature during each test. However, soil temperature must be verified to be equal to the cell temperature. This

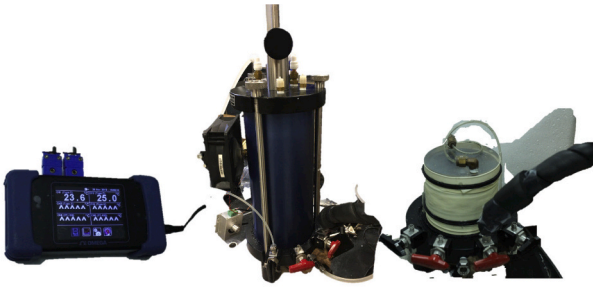

(a) (b) (c)

Fig. 1. Modified cell with different elements: a) Datalogger; b) temperature-controlled cell; c) specimen and the connected tube.

calibration test was performed to determine the time required for the specimen to reach thermal equilibrium. A thin (0.5 mm diameter) *T*-type thermocouple was inserted into the sample using one of the top sample drainage tubes to measure the sample temperature. Both cell and soil temperatures were continuously measured during the thermal loading. The calibration test was conducted for different conditions (e.g. target temperatures). Fig. 2 presents the temperature observations for the calibration test. The results show that the temperature at the core of the soil specimen reaches a steady-state condition (cell temperature) after 40 to 60 min. Therefore, hydraulic conductivity tests at any target temperature were performed at least 60 min after cell temperature was set to that point. Please note, the acrylic chamber in Fig. 2 was only used to show the circulation tube inside the cell. However, for the experiments, as mentioned earlier an aluminum chamber was replaced to avoid any possible failure or unexpected deformation of the acrylic chamber during cyclic thermal loading.

Cell pressure was adjusted and controlled by a digital flow pump connected to the triaxial apparatus. The hydraulic gradient should be controlled to perform hydraulic conductivity tests, and in addition, a higher hydraulic gradient should be used for clay samples, which have low permeability. For this purpose, the second digital flow pump was connected to the bottom port of the sample to apply pressure difference and measure the volume of the water passing through the sample during the H.C. test. The same pump has been used to measure the absorb or expelled water to/from the specimen during the thermal loading until the sample reaches the steady-state condition. The top port of the sample was connected to the standard pressure panel and the pressure was controlled by the panel pressure gauge. The main modification to the setup was to control the temperature of the sample and also to control both the temperature and pressure of the injected water for permeability tests. For the latter purpose, a second water bath was used to accommodate a considerable length of the tube, which connects the pressurized water from the pump to the bottom sample port. With this method, both the temperature and pressure of the water at the inlet port were accurately controlled. It should be mentioned that the measured outflow water (which was collected at the test temperature) was consistent with the inflow water. In the end, the regular acrylic chamber was replaced with an aluminum one, to avoid deformation during several thermal loadings. Fig. 3 shows the full setup, including the standard panel; modified permeameter; and the secondary water bath, which controls the temperature of the injected water, and the two digital flow pumps which one of them provides confining pressure to the cell and the other one which provides pressure and measures the absorbed/expelled water to/from the sample. Please note, in the modified temperature-controlled permeameter, the temperature of the specimen and both the temperature and pressure of the permeant water can be controlled at the same time. Preliminary results and calibration tests determined that a reliable outcome highly depends on the controlled conditions (e.g., sample temperature at the core, uniform cell temperature, and most importantly, the temperature of the injected water). It is important to note that insufficient control in any of these mentioned parameters may lead to a wrong conclusion on the effect of temperature on the permeability of the soil.

3.2. Selected soils

To compare the effects of temperature on permeability and void ratio of both fine and coarse-grained soils, uniform Ottawa sand (SP) and Kaolin clay were selected in this study. Kaolin clay and Ottawa sand have been widely studied in different geotechnical researches as standard fine and granular soils (Darbari et al., 2017; Ghasemi-Fare and Basu, 2018). After finalizing the setup, several permeability tests were performed using both selected soils, and changes in hydraulic conductivity and intrinsic permeability were analyzed. The properties of the Illinois Ottawa sand (washed silica sand) with a majority particle size of 0.425 mm (remained on sieve #40) are presented in Table 1. The particle size distribution of the selected sand is also shown in Fig. 4. In addition, the geotechnical and thermal properties of the Kaolin clay used in this research were measured and are presented in Table 2.

3.3. Sample preparation

Sandy soil was dried in the oven and then was used to fabricate the samples using the dry tamping method inside a latex membrane which was stretched using a two-part vacuum split former with 50.8 mm of diameter. The dry sand was compacted at 3 different layers using a plastic tamper. According to the sample dimensions and the weight of the soil, the initial void ratio was calculated. To prepare clay samples, a compaction mold with a diameter of 101.6 mm was filled with remolded Kaolin clay (compacted specimen), and then the soil was pushed out using a hydraulic jack. A thickness of 25.4 mm was cut using a trimming saw and was placed between the filter papers and porous stones. Please note, since hydraulic conductivity was performed at higher confinement (stress) compared to the initial stress state, all clayey samples were considered as normally consolidated clays. The dimensions of the sample were measured, and the membrane was placed around it. Using the sample dimensions before the test and the dry weight of the soil specimen, the initial void ratio was calculated. After the specimen (Ottawa sand or Kaolin clay) was placed inside the cell, the de-aired water was used to fill the cell and its pressure was set to the target confinement

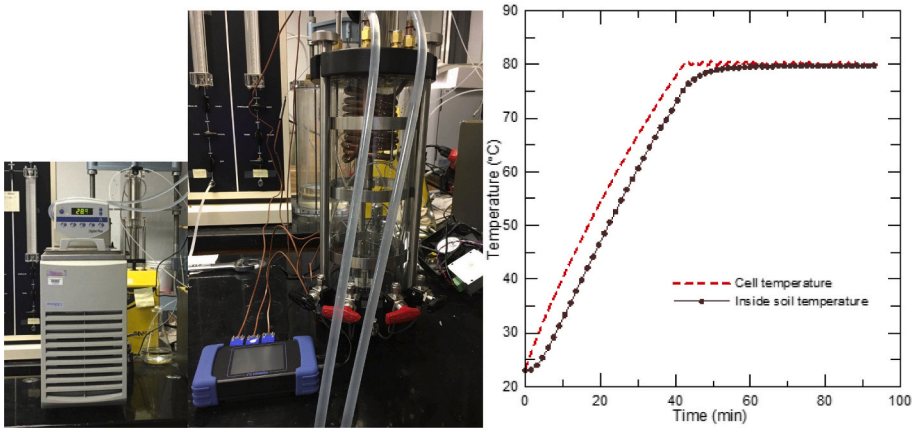

Fig. 2. a) Controlled temperature triaxial permeameter cell; b) Temperature recorded at the cell and the soil center.

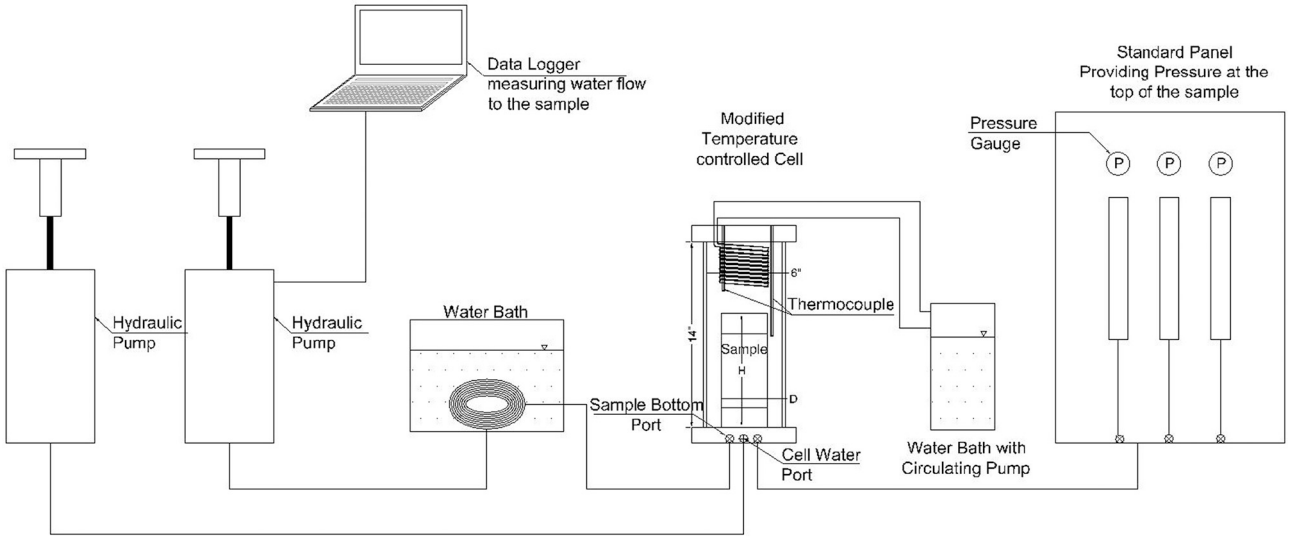

Fig. 3. A schematic view of the complete modified temperature-controlled permeameter cell to perform hydraulic conductivity tests.

Table 1
Geotechnical and thermal properties of Illinois Ottawa silica sand.

G_s	e_{max}	e_{min}	D_{50}	C_c	C_u	α_s[1/°C]	Specific heat capacity of dry Ottawa sand; C_p (J/(kg°C))
2.65	0.86	0.53	0.5 (mm)	0.92	1.02	1.0×10^{-5}	765 (at 20 °C)

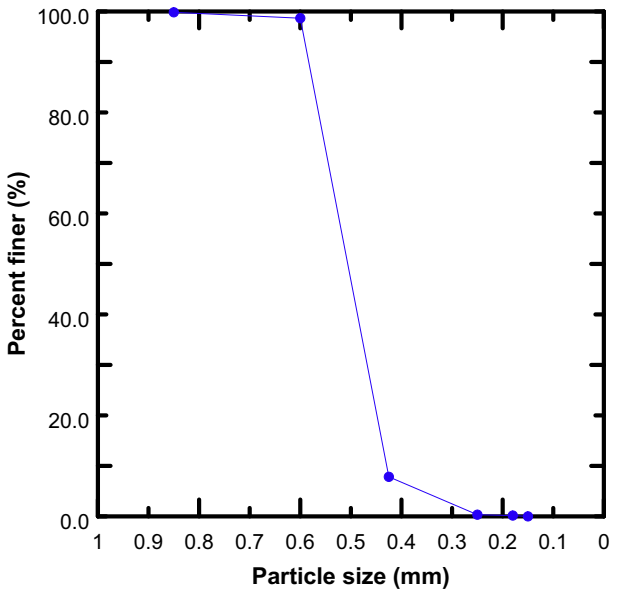

Fig. 4. Particle size distribution for Illinois Ottawa sand.

Table 2
Geotechnical and thermal properties of Columbus Kaolin clay.

Specific Gravity	Plasticity Index	Liquid Limit	VCL Slope (λ)	RCL Slope (κ)	α_s[1/°C]	Specific heat capacity of Kaolinite; C_p (J/(kg°C))
2.65	10	40%	0.228	0.08	2.0×10^{-4}	945 (at 20 °C)

stress. In the next step, the sample was saturated by passing de-aired water through the specimens by applying a pressure gradient between the bottom and the top of the sample. The saturation of the sample was verified before starting each test by measuring Skempton's coefficient B. To assure about reaching the fully saturated condition, cell pressure was increased (70 kPa) and then the changes in the sample pressure were measured to calculate Skempton's coefficient B. The measured B value was greater than 0.97. This value satisfies the saturation requirement which is at least 0.95.

3.4. Test procedure

In the next step, the soil hydraulic conductivity was initially measured at room temperature (20 °C). The cell temperature was then increased to 80 °C through four different steps ($\Delta T = 15$ °C). At each step, the soil hydraulic conductivity was measured at least three times to ensure the repeatability of the tests, and the average value was considered as the hydraulic conductivity at that temperature. The same procedure was repeated at different confinement stresses (different initial void ratios) for both sand and clay. Please note, higher pressure was used to perform permeability tests with a higher hydraulic gradient ($i = 138$) for fine-grained soil (Kaolin clay).

In the final step, the dynamic viscosity of the water (which was tap water in this study) was then measured at each thermal step to analyze the variation of soil intrinsic permeability. A temperature-controlled Rheometer testing device was used to quantify the dynamic viscosity at different temperatures (Please see Fig. 5). The fluid properties at three different temperatures are presented in Table 3. Please note, the calibration of the used Rheometer was verified by comparing the measured dynamic viscosity of the distilled water and the results were very close to the reported values in the literature.

Then, the changes in intrinsic permeability of both Ottawa sand and Kaolin clay were investigated to explore if there were any changes in pore space, and tortuosity (connectivity of the pores) that could be accounted as the soil fabric alterations (e.g., arrangement of particles, particle groups, and pore spaces) with temperature. The soil fabric alterations were not measured directly in this study, however since soil fabric controls the intrinsic permeability, any changes in soil permeability can be interpreted as the result of soil fabric changes.

Fig. 5. The Rheometer was used to measure the dynamic viscosity of water at different temperatures.

Table 3
Dynamic viscosity measurements by the Rheometer.

Temperature (°C)	Measurement from Rheometer (kPa.s)
20	0.00107
50	0.000567
80	0.000378

4. Results

4.1. Effect of temperature on H.C. of Ottawa sand

The results obtained from the hydraulic conductivity test on Ottawa sand at each thermal step are presented in Fig. 6. Fig. 6 presents the hydraulic conductivity variations for Ottawa sand with temperature for different confinement stresses. Please note, as mentioned earlier the hydraulic conductivity that is reported in Fig. 6 at each temperature is the average of the three different tests. The results confirm the repeatability of the experiment under thermal loading using the modified apparatus. Fig. 6 shows that the hydraulic conductivity of Ottawa sand increases by 33% to 37% when the soil temperature is changed from 20 °C to 80 °C. The results which were obtained at different confinement stresses in this study show similar trends with an increase in temperature. Although hydraulic conductivity values were expected to increase at elevated temperatures for sandy soil, as mentioned earlier different rates of changes in hydraulic conductivity were reported in the literature, and consequently, contradictory observations were concluded for

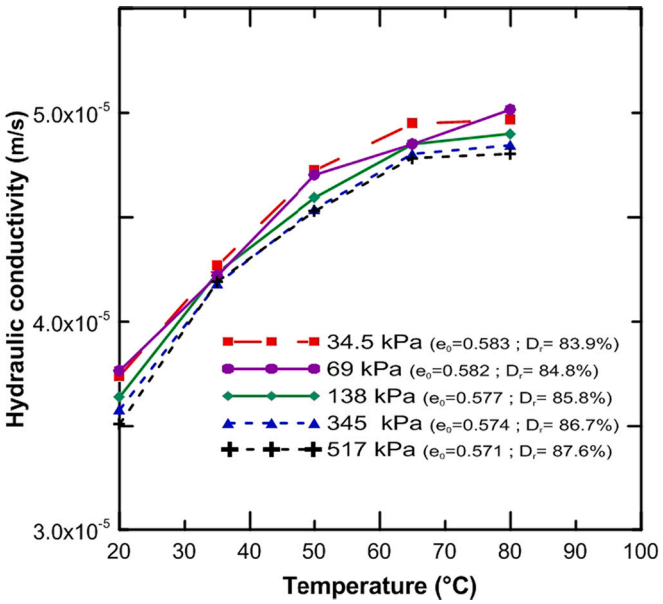

Fig. 6. Variations of hydraulic conductivity of uniform Ottawa sand with the temperature at different confinement stresses.

intrinsic permeability variations with an increase in temperature. Therefore, in the next step, alterations in intrinsic permeability were analyzed by considering the changes in density and dynamic viscosity of the water that were measured at different temperatures.

4.2. Effect of temperature on intrinsic permeability of Ottawa sand

Water density and viscosity are temperature dependent and thus to analyze how much of the change in hydraulic conductivity is due to the volume reduction, or degeneration of adsorbed water into free water (only in clays), the variation in intrinsic permeability of soil should be investigated.

Considering the changes in dynamic viscosity and density of the water, the intrinsic permeability (K) variations with temperature can be calculated using the hydraulic conductivity results ($\kappa = \frac{\gamma_w}{\eta} K$;where η is dynamic viscosity, γ_w is the unit weight of water and κ is hydraulic conductivity).

Fig. 7 presents the changes in the intrinsic permeability of Ottawa sand at different temperatures for five different confinement stresses. By comparing Fig. 6. and Fig. 7, it is interesting to note that, although hydraulic conductivity increases, the intrinsic permeability is reduced by approximately 50% when the soil temperature is raised from 20 °C to 80 °C. Please note, any changes in intrinsic permeability or void ratio of sandy soil with thermal loading can confirm the soil fabric (arrangement of particles, and pore spaces) alterations in sandy soil. Fig. 7 demonstrates almost a linear reduction of intrinsic permeability with temperature. The results show an almost identical reduction in the intrinsic permeability during heating phases for all cases. This reduction in the intrinsic permeability could be a result of void ratio reduction due to thermal loading, and soil densification which can be interpreted as soil fabric changes. Soil fabrics demonstrate the arrangement of particles, particle groups, and pore spaces and controls the ability of the water to flow through the soil (e.g., permeability). Therefore, any changes in intrinsic permeability can be claimed as the soil fabric alterations. Although a wide temperature range (from 20 °C to 80 °C) is considered in this study, similar behavior can be concluded when soil temperature rises from 20 °C to 45 °C which can represent the ranges for ambient temperature fluctuations in summer and soil temperature variation close to geothermal piles. This scenario is valid for the rest of the paper and the presented results can be used for any desired temperature ranges

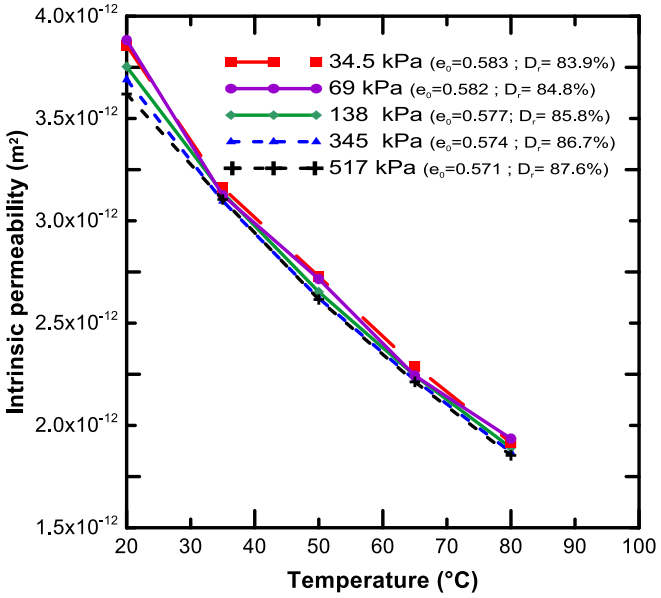

Fig. 7. Variations of intrinsic permeability of Ottawa sand with the temperature at different confinement stresses.

from 20 °C to 80 °C depending on the geographical location or the nature of the problem.Fig. 7

4.3. Effect of temperature on H.C. of Kaolin clay

For the second series of experiments, changes in the permeability of Kaolin clay were studied. Fig. 8 presents the changes in the hydraulic conductivity of Kaolin clay with the temperature at four different confinement stresses. The variation range of hydraulic conductivity at each temperature is also presented using an error bar which are the results of the three repeated tests at each thermal step. Please note, the error bar in this figure simply shows the ranges of hydraulic conductivity values measured at three different tests. The results show that the hydraulic conductivity of Kaolin clay increases by approximately 155% when the temperature increased from 20 °C to 80 °C. Comparison of Fig. 6 and Fig. 8 demonstrates that the changes in the hydraulic conductivity of Kaolin clay with temperature are significantly higher than that of Ottawa sand. To better understand this comparison, the changes in the intrinsic permeability of Kaolin clay were analyzed.

4.4. Effect of temperature on the intrinsic permeability of Kaolin clay

Considering the dynamic viscosity and density variations of the water with temperature, the intrinsic permeability values of Kaolin clay at different temperatures were calculated. Fig. 9 presents the changes in the intrinsic permeability of Kaolin clay with temperature. Results determine a slight reduction (less than 4%) under 69 kPa confinement and almost no changes for higher confinements in the intrinsic permeability after the temperature raised to 80 °C. This lower amount of

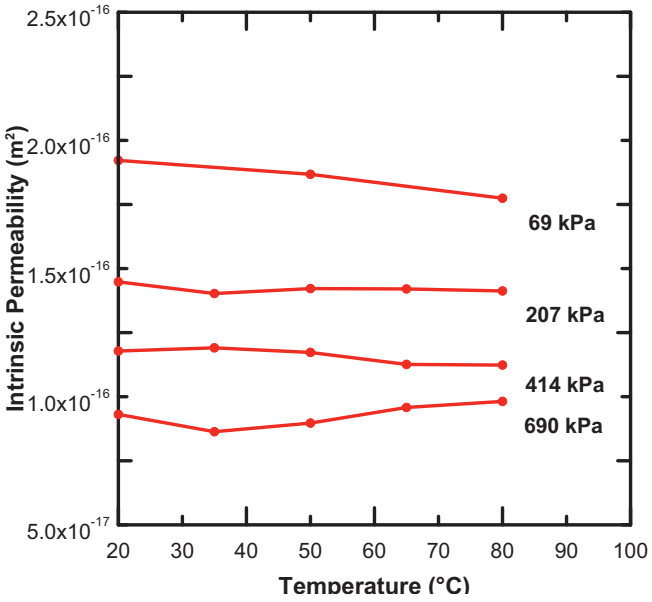

Fig. 9. Variations of intrinsic permeability of Kaolin clay during heating at different confinement stresses.

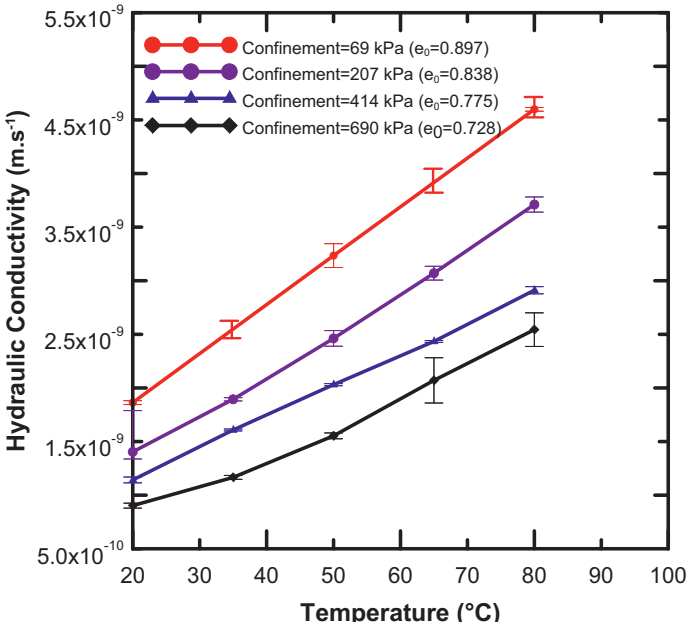

Fig. 8. Changes in hydraulic conductivity of Kaolin clay with the temperature at different confinement stresses.

reduction in intrinsic permeability compared to Ottawa sand under the same conditions could be because of the degeneration of a part of the adsorbed water into the free water in clays at the elevated temperatures that is reported in the literature (Derjaguin et al., 1986; Ma and Hueckel, 1993; Seiphoori, 2015). In the next section, the thermal volume changes of both Ottawa sand and Kaolin clay are investigated to explore if the changes in intrinsic permeability in both materials are consistent with the void ratio changes with thermal loading.

5. Discussion

5.1. Volumetric change

Changes in void ratio with temperature were also studied in this research. Volumetric and void ratio variations with temperature were calculated by monitoring and measuring the amount of expelled water during thermal loading. Campanella and Mitchell (1968) proposed a relation (Eq. 1) between drained (or absorbed) water (ΔV_{dr}) and thermal expansion of the water and solid parts to predict the thermal volume change of the specimen (ΔV_m). Thermal volume change or consequently the changes in void ratio can alternatively be measured by monitoring the changes in volume of the water inside the cell and calibration of the measurements considering the effects of temperature on the equipment made with aluminum.

$$(\Delta V_{dr})_{\Delta T} = \alpha_w V_w \Delta T + \alpha_s V_s \Delta T - (\Delta V_m)_{\Delta T} \quad (1)$$

where α_w and α_s are, respectively, the coefficient of thermal expansion of the water and soil; and $V_w(=V_v)$ and V_s are, respectively, initial pore water volume (equal to void volume) and soil grains volume before each thermal step.

During thermal loading, the amount of water expelled or absorbed by the sample was measured, and since the initial amounts for V_w and V_s were known, change in the volume of the specimen (ΔV_m) was calculated from Eq. (1) at each thermal loading step ($\Delta T = 15$ °C) and was used to calculate the new amount for $V_w(=V_v)$, considering the changes in soil grains volume. Calculated values for V_w and V_s, were used as the initial pore water and solid grains volumes for the next thermal loading step. The coefficient of thermal expansion of water (α_w) was considered variable depending on the temperature of each load step ranging between 2.07×10^{-4} [1/°C] for 20 °C to 6.40×10^{-4} [1/ °C] for 80 °C. Coefficient of thermal expansion for silica sand (α_s) and for Kaolin clay were considered to be equal to 1.0×10^{-5} [1/ °C], and 2.0×10^{-4} [1/ °C], respectively (McKinstry, 1965). Void ratio values were determined using calculated (updated) V_w and V_s after each thermal load. The calculated void ratio variations with temperature during heating for Ottawa sand and Kaolin clay are presented in Fig. 10. Comparing Figs. 10(a) and 10(b) depict that 4% and 7% reductions in the void ratio were recorded, respectively, for Ottawa sand and Kaolin clay when soil temperature increased from 20 °C to 80 °C. It is to be noted that, Delage et al. (2009) also observed almost similar thermal volume contraction in Boom clay and reported that porosity decreases from 39% ($e = 0.64$) to 37.2% ($e = 0.59$) (6 to 7% void ratio reduction) when soil temperature raised from 20 °C to 90 °C.

Experimental results presented in this study confirm that increase in temperature will alter soil hydraulic conductivity and intrinsic permeability. This happens not only because of fluid density and viscosity variations with temperature; thermal loading alters the pore spaces in both sand and clay and consequently could change soil fabric. It is interesting to note that, although thermal loading induces void ratio reduction in both Ottawa sand and Kaolin clay, the intrinsic permeability alterations with temperature in the studied sand and clay were different. The intrinsic permeability of Ottawa sand reduces by approximately 50% in all confinement stresses during the heating cycle from 20 °C to 80 °C. The reduction in intrinsic permeability in sandy soil is due to the particle rearrangement and reduction in a void ratio (volumetric change), as shown in Fig. 10 (a).

Interestingly, although the void ratio decrease in Kaolin clay is more distinct during the heating cycle compared to Ottawa sand, the intrinsic permeability of Kaolin clay shows almost no changes or slightly reduces under lower confinement (e.g., at 69 kPa) for the same thermal loading (temperature changes from 20 °C to 80 °C). Since the intrinsic permeability is a function of porous media and the decrease in void ratio supports for a reduction in intrinsic permeability, there should be another mechanism that causes to get higher H.C values and accordingly lower changes in intrinsic permeability at elevated temperatures in Kaolin clay compared to Ottawa sand. According to the literature, an increase in the flow channels due to the degeneration of the water from the interlayer pores into the free water (bulk water) at elevated

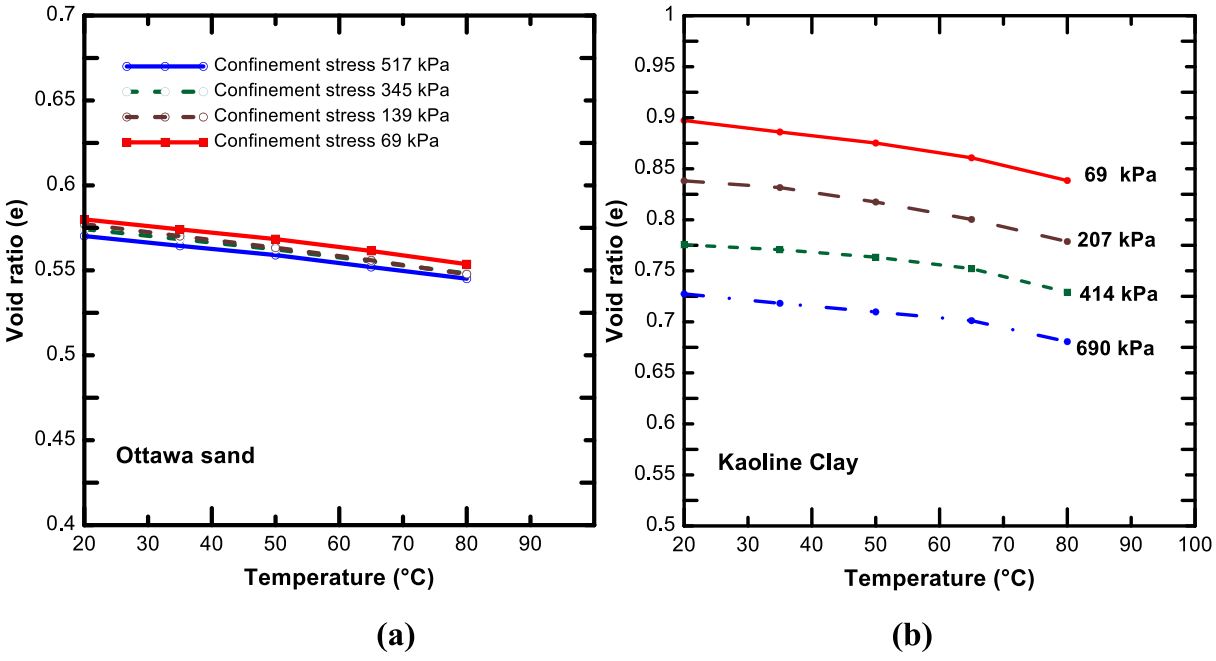

Fig. 10. Void ratio alterations with the temperature at different confinement stresses (a) Ottawa sand during heating load; and (b) Kaolin clay during heating load.

temperatures are identified as one of the reasons for the increased permeability (Derjaguin, 1986; Pusch and Güven, 1990; Seiphoori, 2015). This can be a justification for the different observations on the effect of temperature on the intrinsic permeability of Ottawa sand and Kaolin clay. Indeed, in this condition, changes in the void ratio do not have a direct relation with permeability. Ma and Hueckel (Ma and Hueckel, 1993) also mentioned that thermal energy may induce a mechanism in which a part of the immobile water within the structure moves into the mobile water and, therefore, permeability increases.

5.2. Comparison with the Kozeny-Carman equation

To investigate if the Kozeny-Carman equation can be used to estimate the hydraulic conductivity of sandy soils at elevated temperatures by only considering void ratio changes with temperature, the difference between the measured and calculated hydraulic conductivity using the Kozeny-Carman equation were compared. According to the Kozeny-Carman equation, hydraulic conductivity for sandy soil can be predicted using Eq. (2).

$$\kappa = \frac{1}{C_s S_s \Gamma}\frac{\gamma_w}{\eta}\frac{e^3}{1+e} \tag{2}$$

where: k is hydraulic conductivity; C_s is shape factor (which is a function of the shape of flow channels); S_s is the specific surface area per unit volume of particles; Γ is tortuosity of flow channels; γ_w is the unit weight of the water;η is the dynamic viscosity of the permeant, and e is the void ratio.

In order to explore the importance of considering the variations of tortuosity, specific area, and shape factor (in general soil fabric) at elevated temperatures, at this step only the changes in void ratio with temperature were considered. As discussed above, at each thermal loading step in the experiment, void ratio, unit weight, and dynamic viscosity were measured (please see Fig. 10, and Table 3). Therefore, the product of the $C_s \times S_s \times \Gamma$ can be calculated using Eq. (3) and by utilizing the hydraulic conductivity measured at room temperature (20 °C).

$$C_s S_s \Gamma = \frac{1}{\kappa_1}\frac{\gamma_{w_1}}{\eta_1}\frac{e_1^3}{1+e_1} \tag{3}$$

where, κ_1 is the initial hydraulic conductivity measured at room temperature, γ_{w1}, and η_1 are the unit weight and dynamic viscosity of the water at 20 °C, and e_1, is the initial void ratio.

Then the hydraulic conductivity at any temperature could be predicted by substituting Eq. (3) in Eq. (2) and using the initial hydraulic conductivity which was measured at room temperature (20 °C) (Eq. 4).

$$\kappa_2 = \left(\frac{1}{\frac{1}{\kappa_1}\frac{\gamma_{w_1}}{\eta_1}\frac{e_1^3}{1+e_1}}\right)\times\frac{\gamma_{w_2}}{\eta_2}\frac{e_2^3}{1+e_2} = \kappa_1 \times \frac{\frac{\gamma_{w_2}}{\eta_2}}{\frac{\gamma_{w_1}}{\eta_1}}\frac{\frac{e_2^3}{1+e_2}}{\frac{e_1^3}{1+e_1}} \tag{4}$$

where κ_2 is the hydraulic conductivity at temperature (T_2) and κ_1 is the hydraulic conductivity measured at 20 °C. According to Eq. (4), the hydraulic conductivity at elevated temperatures can be predicted by measuring the changes in the void ratio at two thermal steps. The comparisons between the measured and calculated hydraulic conductivity for four different confinement stresses are presented in Table 4. As can be seen in Table 4, the percentage of error increases at elevated temperatures if only thermal void ratio reduction is considered. This clearly confirms that considering a constant value for $C_s \times S_s \times \Gamma$ (constant values for tortuosity, shape factor, and specific area) at variable temperatures is not correct and we expect tortuosity, specific area, and shape factor to be varied at elevated temperatures.

Tortuosity, void ratio, and shape of the flow channel depend on the geometry of the particles, arrangement of soil particles, particle groups, and pore spaces in the medium. Thermal loading induces volume change and therefore it densifies the soil sample by rearranging the soil particles and making their positions different from the initial condition. In addition, when the water inside the pores expands at higher temperatures, the extra water will be expelled (dissipated) from the specimen and the movement of water may also facilitate soil particles rearrangement (Joshaghani and Ghasemi-Fare, 2021; Tamizdoust and Ghasemi-Fare, 2021). This explains the physics of the permeability variations in Ottawa sand with thermal loading and considering of updated tortuosity, void ratio, and shape of the flow channel at elevated temperatures. Please note, thermal loading has been also considered as one of the ground modification techniques for clayey soils which is known as thermal consolidation (Cherati and Ghasemi-Fare, 2021; Tamizdoust

Table 4
Comparison of measured and calculated intrinsic permeability of Ottawa sand using Kozeny-Carman equation at different temperatures and confinement stresses

Temperature (°C)	Measured κ (m/s)	Measured K (m^2)	$\frac{e^3}{(1+e)}$	$\frac{\gamma_w}{(\eta)}$ (1/m.s)	Calculated κ based on Eq. 2 (m/s)	Calculated K based on Eq. 2 (m2)	Differences (%)
Confinement stress = 69 kPa							
20	3.74E-05	3.86E-12	0.1235	9,694,903.549	3.74E-05	3.86E-12	0.00
35	4.27E-05	3.16E-12	0.1202	13,506,711.03	2.61E-05	1.93E-12	−38.79
50	4.72E-05	2.73E-12	0.1171	17,318,518.52	1.98E-05	1.15E-12	−57.99
65	4.95E-05	2.29E-12	0.1133	21,618,253.33	1.54E-05	7.12E-13	−68.9
80	4.97E-05	1.92E-12	0.1092	25,917,988.13	1.24E-05	4.77E-13	−75.09
Confinement stress = 138 kPa							
20	3.64E-05	3.75E-12	0.1219	9,694,903.549	3.64E-05	3.75E-12	0.00
35	4.24E-05	3.14E-12	0.1180	13,506,711.03	2.53E-05	1.87E-12	−40.30
50	4.59E-05	2.65E-12	0.1144	17,318,518.52	1.91E-05	1.10E-12	−58.41
65	4.85E-05	2.24E-12	0.1104	21,618,253.33	1.48E-05	6.84E-13	−69.53
80	4.90E-05	1.89E-12	0.1061	25,917,988.13	1.18E-05	4.57E-13	−75.82
Confinement stress = 345 kPa							
20	3.58E-05	3.69E-12	0.1203	9,694,903.549	3.58E-05	3.69E-12	0.00
35	4.18E-05	3.10E-12	0.1171	13,506,711.03	2.50E-05	1.85E-12	−40.25
50	4.54E-05	2.62E-12	0.1138	17,318,518.52	1.90E-05	1.09E-12	−58.26
65	4.80E-05	2.22E-12	0.1101	21,618,253.33	1.47E-05	6.79E-13	−69.44
80	4.84E-05	1.87E-12	0.1064	25,917,988.13	1.18E-05	4.57E-13	−75.57
Confinement stress = 517 kPa							
20	3.51E-05	3.62E-12	0.1181	9,694,903.549	3.51E-05	3.62E-12	0.00
35	4.19E-05	3.10E-12	0.1149	13,506,711.03	2.45E-05	1.82E-12	−41.52
50	4.53E-05	2.62E-12	0.1120	17,318,518.52	1.86E-05	1.08E-12	−58.85
65	4.78E-05	2.21E-12	0.1083	21,618,253.33	1.44E-05	6.68E-13	−69.81
80	4.80E-05	1.85E-12	0.1048	25,917,988.13	1.17E-05	4.50E-13	−75.74

and Ghasemi-Fare, 2020c). The same physics and densification can explain the thermal consolidation phenomenon.

Therefore, it can be concluded that the Kozeny-Carman equation can only be used if the changes in void ratio as well as tortuosity, specific area, and shape factor are accurately measured at elevated temperatures with the changes in soil fabric (arrangement of particle groups and pore spaces).

6. Conclusion

In this research, a temperature-controlled triaxial permeameter cell was modified to analyze the variations of intrinsic permeability and the volumetric changes of sandy and clayey soils with temperature under different confinement stresses. Several calibration tests were conducted to prepare the final setup. Results confirmed that changes in the temperature alter not only the soil hydraulic conductivity but also the intrinsic permeability. This happens because thermal loading changes the soil fabric (e.g., soil particle rearrangements and void ratio changes) and porosity in both sand and clay. Experimental observations through a temperature-controlled permeameter cell confirmed a 35% increase in hydraulic conductivity of the saturated sandy soil. However, considering fluid properties (e.g., density and dynamic viscosity) variation with temperature, a 50% reduction in intrinsic permeability was observed for the saturated sand. This reduction in intrinsic permeability happens due to a decrease in void ratio and volume contraction of the soil specimen during the thermal loading. The void ratio variations with temperature during the thermal loading cycles were measured based on the volume of the expelled and absorbed water, and the estimated amount of volume expansion and contraction according to the initial water content. Thermal loading in the ground resulted in different behaviors for sand and clay. In sandy soil, void ratio reduction with temperature increase caused lower intrinsic permeability. However, the results for clayey soil, indicate a slight reduction (less than 4%) in intrinsic permeability under low confinement (e.g. 69 kPa) and show almost no changes for higher confinements when the temperature rises from 20 °C to 80 °C despite the void ratio reduction. This happened because, at elevated temperatures, a part of the immobile water within the structure could move into the mobile water to increase the flow channels.

Data availability

All data, models, and code generated or used during the study appear in the submitted article.

Declaration of Competing Interest

The authors declare that they have no known competing financial interests or personal relationships that could have appeared to influence the work reported in this paper.

Acknowledgements

The authors would also like to gratefully acknowledge the financial support of the National Science Foundation under Grant No. CMMI-1804822.

References

Aktan, T., Ali, S., 1975. Effect of Cyclic and In Situ Heating on the Absolute Permeabilities, Elastic Constants, and Electrical Resistivities of Rocks. Fall Meeting of the Society of Petroleum Engineers of AIME. Society of Petroleum Engineers.

Arihara, N., 1974. A study of non-isothermal single and two-phase flow through consolidated sandstones. In: Stanford Geothermal Program. Stanford Univ., CA (USA).

Aruna, M., 1977. The Effects of Temperature and Pressure on Absolute Permeability of Sandstones. American Nuclear Society Topical Meeting Golden.

Campanella, R.G., Mitchell, J.K., 1968. Influence of temperature variations on soil behavior. Journal of Soil Mechanics & Foundations Div 94 (3), 9–22. https://doi.org/10.1061/JSFEAQ.0001136.

Chen, W., Ma, Y., Yu, H., Li, F., Li, X., Sillen, X., 2017. Effects of temperature and thermally-induced microstructure change on hydraulic conductivity of Boom Clay. J. Rock Mech. Geotech. Eng. 9, 383–395.

Cherati, D.Y., Ghasemi-Fare, O.J.G., 2019. Analyzing transient heat and moisture transport surrounding a heat source in unsaturated porous media using the Green's function, 81, pp. 224–234.

Cherati, D.Y., Ghasemi-Fare, O., 2021. Unsaturated thermal consolidation around a heat source. Comput. Geotech. 134, 104091.

Cho, W., Lee, J., Chun, K., 1999. The temperature effects on hydraulic conductivity of compacted bentonite. Appl. Clay Sci. 14, 47–58.

Damiano, E., Greco, R., Guida, A., Olivares, L., Picarelli, L., 2017. Investigation on rainwater infiltration into layered shallow covers in pyroclastic soils and its effect on slope stability. Engineering Geology 220.

Darbari, Z., Jaradat, K.A., Abdelaziz, S.L., 2017. Heating–freezing effects on the pore size distribution of a kaolinite clay. Environ. Earth Sci. 76, 713.

Delage, P., Sultan, N., Cui, Y.J., 2000. On the thermal consolidation of Boom clay. Can. Geotech. J. 37, 343–354.

Delage, P., Sultan, N., Cui, Y.-J., Ling, L.X., 2009. Permeability changes in Boom clay with temperature. International Conference and Workshop "Impact of Thermo-Hydro-Mechanical-Chemical (THMC) processes on the safety of underground radioactive waste repositories", European Union 331–335.

Derjaguin, B.J.F.i.p, 1986. Properties of water layers adjacent to interfaces, pp. 663–738.

Derjaguin, B., Karasev, V., Khromova, E.J.J.o.c. & science, i, 1986. Thermal Expansion of Water in Fine Pores, 109, pp. 586–587.

Dou, H.-Q., Han, T.-C., Gong, X.-N., Zhang, J., 2014. Probabilistic slope stability analysis considering the variability of hydraulic conductivity under rainfall infiltration–redistribution conditions. Eng. Geol. 183, 1–13.

François, B., Laloui, L., Laurent, C., 2009. Thermo-hydro-mechanical simulation of ATLAS in situ large scale test in Boom Clay. Comput. Geotech. 36, 626–640.

Gao, H., Shao, M., 2015. Effects of temperature changes on soil hydraulic properties. Soil Tillage Res. 153, 145–154.

Garakani, A.A., Haeri, S.M., Khosravi, A., Habibagahi, G., 2015. Hydro-mechanical behavior of undisturbed collapsible loessial soils under different stress state conditions. Eng. Geol. 195, 28–41.

Ghasemi-Fare, O., Basu, P., 2015. Numerical modeling of thermally induced pore water flow in saturated soil surrounding geothermal piles. IFCEE 2015, 1668–1677.

Ghasemi-Fare, O., Basu, P., 2018. Influences of ground saturation and thermal boundary condition on energy harvesting using geothermal piles. Energy and Buildings 165, 340–351.

Ghasemi-Fare, O., Basu, P., 2019. Coupling heat and buoyant fluid flow for thermal performance assessment of geothermal piles. Comput. Geotech. 116, 103211.

Gobran, B., Brigham, W., Ramey Jr., H., 1987. Absolute permeability as a function of confining pressure, pore pressure, and temperature. SPE Form. Eval. 2, 77–84.

Greenberg, D.B., Cresap, R.S., Malone, T.A., 1968. Intrinsic permeability of hydrological porous mediums: Variation with temperature. Water Resour. Res. 4, 791–800.

Habibagahi, K., 1977. Temperature effect and the concept of effective void ratio. Indian Geotechnical Journal 7, 14–34.

Hillel, D., 2013. Fundamentals of Soil Physics. Academic press.

Jefferson, I., Rogers, C.D.F., 1998. Liquid limit and the temperature sensitivity of clays. Eng. Geol. 49, 95–109.

Joshaghani, M., Ghasemi-Fare, O., 2019. A Study on thermal consolidation of fine grained soils using modified triaxial cell. In: Eighth International Conference on Case Histories in Geotechnical Engineering. ASCE, Philadelphia, Pennsylvania, pp. 148–156.

Joshaghani, M., Ghasemi-Fare, O., 2021. Experimental Study to Analyze the effect of Confinement and Cell pressure on thermal Pressurization under fully Undrained Conditions, 2021. IFCEE, pp. 274–281.

Joshaghani, M., Ghasemi-Fare, O., Ghavami, M., 2018. Experimental Investigation on the effects of temperature on physical properties of sandy soils. IFCEE 675–685.

Leung, A., Feng, S., Vitali, D., Ma, L., Karimzadeh, A.J.J., Engineering, G, 2020. Temperature Effects on the Hydraulic Properties of Unsaturated Sand and Their Influences on Water-Vapor Heat Transport, 146, p. 06020003.

Ma, C., Hueckel, T., 1993. Thermomechanical effects on adsorbed water in clays around a heat source. International journal for numerical analytical methods in geomechanics 17, 175–196.

McKinstry, H.A., 1965. Thermal expansion of clay minerals. American Mineralogist: Journal of Earth Planetary Materials 50, 212–222.

Monfared, M., Sulem, J., Delage, P., Mohajerani, M., 2014. Temperature and damage impact on the permeability of Opalinus clay. Rock Mech. Rock. Eng. 47, 101–110.

Morin, R., Silva, A., 1984. The effects of high pressure and high temperature on some physical properties of ocean sediments. Journal of Geophysical Research: Solid Earth 89, 511–526.

Ng, C.W.W., Leung, A.K., 2012. In-situ and laboratory investigations of stress-dependent permeability function and SDSWCC from an unsaturated soil slope. Geotech. Eng. 43, 26–39.

Pusch, R., 1992. Use of bentonite for isolation of radioactive waste products. Clay Miner. 27, 353–361.

Pusch, R., Güven, N., 1990. Electron microscopic examination of hydrothermally treated bentonite clay. Eng. Geol. 28, 303–314.

Ren, J., Shen, Z.-Z., Yang, J., Zhao, J., Yin, J.-N., 2014. Effects of temperature and dry density on hydraulic conductivity of silty clay under infiltration of low-temperature water. Arabian Journal for Science Engineering Geology 39, 461–466.

Romero, E., Gens, A., Lloret, A., 2001. Temperature effects on the hydraulic behaviour of an unsaturated clay. In: Unsaturated Soil Concepts and Their Application in Geotechnical Practice. Springer, pp. 311–332.
Sadeghi, H., AliPanahi, P., 2020. Saturated hydraulic conductivity of problematic soils measured by a newly developed low-compliance triaxial permeameter. Engineering Geology 105827.
Sageev, A., 1980. The Design and Construction of an Absolute Permeameter to Measure the Effect of Elevated Temperature on the Absolute Permeability to Distilled Water of Unconsol Idated Sand Cores. Stanford Geothermal Program.
Seiphoori, A., 2015. Thermo-Hydro-Mechanical Characterisation and Modelling of Wyoming Granular Bentonite. Nagra.
Somerton, W., Gupta, V., 1965. Role of fluxing agents in thermal alteration of sandstones. J. Pet. Technol. 17, 585–588.
Tamizdoust, M.M., Ghasemi-Fare, O., 2020a. Comparison of thermo-poroelastic and thermo-poroelastoplastic constitutive models to analyze THM process in clays. In: E3S Web of Conferences. EDP Sciences, p. 04008.
Tamizdoust, M.M., Ghasemi-Fare, O., 2020b. Coupled thermo-hydro-mechanical modeling of saturated Boom clay. In: Geo-Congress 2020: Geo-Systems, Sustainability, Geoenvironmental Engineering, and Unsaturated Soil Mechanics. American Society of Civil Engineers Reston, VA, pp. 340–348.
Tamizdoust, M.M., Ghasemi-Fare, O., 2020c. A fully coupled thermo-poro-mechanical finite element analysis to predict the thermal pressurization and thermally induced pore fluid flow in soil media. Comput. Geotech. 117, 103250.
Tamizdoust, M.M., Ghasemi-Fare, O., 2021. Assessment of Thermo-Osmosis effect on thermal Pressurization in Saturated Porous Media. IFCEE 2021, 99–108.
Towhata, I., Kuntiwattanaku, P., Seko, I., Ohishi, K., 1993. Volume change of clays induced by heating as observed in consolidation tests. Soils Found. 33, 170–183.
Villar, M.V., Lloret, A.J.A.C.S., 2004. Influence of temperature on the hydro-mechanical behaviour of a compacted bentonite, 26, pp. 337–350.
Weinbrandt, R., Ramey Jr., H., Casse, F., 1975. The effect of temperature on relative and absolute permeability of sandstones. Soc. Pet. Eng. J. 15, 376–384.
Ye, W.-M., Wan, M., Chen, B., Chen, Y.-G., Cui, Y.-J., Wang, J., 2012. Temperature effects on the unsaturated permeability of the densely compacted GMZ01 bentonite under confined conditions. Eng. Geol. 126, 1–7.
Ye, W.-M., Wan, M., Chen, B., Chen, Y., Cui, Y., Wang, J., 2013. Temperature effects on the swelling pressure and saturated hydraulic conductivity of the compacted GMZ01 bentonite. Environ. Earth Sci. 68, 281–288.